A Method for Calculating the Dynamic Stability of a Human-Piloted Airplane by the "Root-Locus Method"

By

Hiroshi MAEDA*

(Received January 23, 1961)

A method of treating a human-piloted airplane as one closed-loop system and calculating the dynamic stability of the airplane by the Evans's "Root-Locus Method" has been investigated.

Using this method, not only the characteristics of the transient motion but also the control ability of the human-pilot to decrease the residual motion of the airplane can be understood conveniently.

In this paper, some results of numerical calculation with this method are described for a typical airplane.

1. Introduction

In the analysis of the dynamic stability of a human-piloted airplane, it is customary of treat the airplane as one element of an open-loop system. However, in the same way as with an airplane equipped with an autopilot or autostabilizer, it is possible to calculate the stability of an airplane as a closed-loop system which contains a human-pilot as one feedback element.

When an airplane is treated as a closed-loop system, it will be convenient to understand not only the transient motion characteristics but the control ability of the human-pilot to decrease the residual motion of the airplane. In order to investigate the characteristics of the transient response of a dynamic system, it is most convenient to trace the root locus of the system characteristic equation. Therefore, the Evans's "Root-Locus Method" has been applied in this paper to to calculate the dynamic stability of an airplane.

Nevertheless, the transfer function for a human-pilot as one control element of an automatic control system will be difficult to establish, but, in this paper, the relatively simple forms have been assumed as a first trial.

* Department of Aeronautical Engineering

2. Transfer Functions of Open-Loop Element

The principle of the Evans's "Root-Locus Method" is described as follows: The root locus of the characteristic equation of a closed-loop system can be determined graphically from the zeros and poles of the transfer function of the open loop elements.

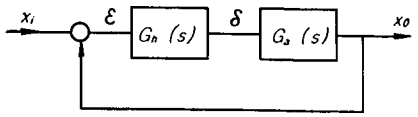

Fig. 1. Closed-loop for a human-piloted airplane.

In the first place, therefore, it is necessary to determine the transfer function of each open-loop element as a polynomial form. As shown in Fig. 1, the closed-loop system includes an airplane and a human-pilot as the open-loop elements.

(1) Determination of the airplane transfer function $G_a(s)$

The transfer function $G_a(s)$ can be determined from the longitudinal and lateral equations of motion of the airplane. These equations are expressed as follows[1]:

$$(2\mu D - C_{xu})\,\hat{u} - C_{x\alpha}\cdot\alpha + C_{L0}\cdot\theta = 0 \tag{1}$$

$$(2C_{L0} - C_{zu})\,\hat{u} + (2\mu D - C_{z\dot{\alpha}}\cdot D - C_{z\alpha})\,\alpha - (2\mu + C_{zq})\,D\theta = C_{z\eta}\cdot\eta \tag{2}$$

$$-C_{mu}\cdot\hat{u} - (C_{m\dot{\alpha}}\cdot D + C_{m\alpha})\,\alpha + (i_B D^2 - C_{mq}D)\,\theta = C_{m\eta}\cdot\eta \tag{3}$$

$$\mu = \frac{m}{\rho s l^3} \qquad i_B = \frac{B}{\rho s l^5}$$

$$t^* = \frac{l}{u_0} \qquad l = \frac{c}{2}$$

$$(2\mu D - C_{y\beta})\,\beta - (C_{yp}D + C_{L0})\,\phi + (2\mu - C_{yr})\,D\psi = 0 \tag{4}$$

$$-C_{l\beta}\cdot\beta + (i_A D^2 - C_{lp}\cdot D)\,\phi - (i_E D + C_{lr})\,D\psi = C_{l\xi}\cdot\xi + C_{l\zeta}\cdot\zeta \tag{5}$$

$$-C_{n\beta}\cdot\beta - (i_E D^2 + C_{np}\cdot D)\,\phi + (i_C D - C_{nr})\,D\psi = C_{n\xi}\cdot\xi + C_{n\zeta}\cdot\zeta \tag{6}$$

$$\mu = \frac{m}{\rho s l^3} \qquad i_A = \frac{A}{\rho s l^5} \qquad i_C = \frac{C}{\rho s l^5}$$

$$i_E = \frac{E}{\rho s l^4} \qquad t^* = \frac{l}{u_0} \qquad l = \frac{b}{2}$$

The above-mentioned equations are given in the nondimensional form and the flight path is assumed to be horizontal ($\theta_0 = 0$).

The transfer functions of the longitudinal motion can be calculated from the longitudinal equations of motion (1), (2) and (3) as follows:

$$G_{\alpha\eta}(s) = \frac{D_1}{D} \tag{7}$$

$$G_{\theta\eta}(s) = \frac{D_2}{D} \tag{8}$$

where

$$D = \begin{vmatrix} 2\mu s - C_{xu} & -C_{x\alpha} & C_{L0} \\ 2C_{L0} - C_{zu} & 2\mu s - C_{z\dot{\alpha}} \cdot s - C_{z\alpha} & -(2\mu + C_{zq})\, s \\ -C_{mu} & -(Cm_{\dot{\alpha}} \cdot s + C_{m\alpha}) & i_B s^2 - C_{mq} \cdot s \end{vmatrix} \tag{9}$$

$$D_1 = \begin{vmatrix} 2\mu s - C_{xu} & 0 & C_{L0} \\ 2C_{L0} - C_{zu} & C_{z\eta} & -(2\mu + C_{zq})\, s \\ -C_{mn} & C_{m\eta} & i_B s^2 - C_{mq} \cdot s \end{vmatrix} \tag{10}$$

$$D_2 = \begin{vmatrix} 2\mu s - C_{xu} & -C_{x\alpha} & 0 \\ 2C_{L0} - C_{zu} & 2\mu s - C_{z\dot{\alpha}} \cdot s - C_{z\alpha} & C_{z\eta} \\ -C_{mu} & -(C_{m\dot{\alpha}} \cdot s + C_{m\alpha}) & C_{m\eta} \end{vmatrix} \tag{11}$$

In the same way as the above-mentioned cases, the transfer functions of the lateral motion can be determined from the lateral equations of motion (4), (5) and (6) as follows:

$$G_{\beta\xi}(s) = \frac{D_1'}{D'} \tag{12}$$

$$G_{\phi\xi}(s) = \frac{D_2'}{D'} \tag{13}$$

$$G_{\psi\xi}(s) = \frac{D_3'}{D'} \tag{14}$$

$$G_{\beta\zeta}(s) = \frac{D_4'}{D} \tag{15}$$

$$G_{\phi\zeta}(s) = \frac{D_5'}{D'} \tag{16}$$

$$G_{\psi\zeta}(s) = \frac{D_6'}{D'} \tag{17}$$

where

$$D' = \begin{vmatrix} 2\mu s - C_{y\beta} & -(C_{yp} s + C_{L0}) & (2\mu - C_{yr})\, s \\ -C_{l\beta} & i_A s^2 - C_{lp} s & -(i_E s + C_{lr})\, s \\ -C_{n\beta} & -(i_E s^2 + C_{np} s) & (i_C s - C_{nr})\, s \end{vmatrix} \tag{18}$$

$$D_1' = \begin{vmatrix} 0 & -(C_{yp} s + C_{L0}) & (2\mu - C_{yr})\, s \\ C_{l\xi} & i_A s^2 - C_{lp} s & -(i_E s + C_{lr})\, s \\ C_{n\xi} & -(i_E s^2 + C_{np} s) & (i_C s - C_{nr})\, s \end{vmatrix} \tag{19}$$

$$D_2' = \begin{vmatrix} 2\mu s - C_{y\beta} & 0 & (2\mu - C_{yr})\, s \\ -C_{l\beta} & C_{l\xi} & -(i_E s + C_{lr})\, s \\ -C_{n\beta} & C_{n\xi} & (i_C s - C_{nr})\, s \end{vmatrix} \tag{20}$$

$$D_3' = \begin{vmatrix} 2\mu s - C_{y\beta} & -(C_{yp}s + C_{L0}) & 0 \\ -C_{l\beta} & i_A s^2 - C_{lp}s & C_{l\xi} \\ -C_{n\beta} & -(i_E s^2 + C_{np}s) & C_{n\xi} \end{vmatrix} \tag{21}$$

$$D_4' = \begin{vmatrix} 0 & -(C_{yp}s + C_{L0}) & (2\mu - C_{yr})s \\ C_{l\zeta} & i_A s^2 - C_{lp}s & -(i_E s + C_{lr})s \\ C_{n\zeta} & -(i_E s^2 + C_{np}s) & (i_C s - C_{nr})s \end{vmatrix} \tag{22}$$

$$D_5' = \begin{vmatrix} 2\mu s - C_{y\beta} & 0 & (2\mu - C_{yr})s \\ -C_{l\beta} & C_{l\zeta} & -(i_E s + C_{lr})s \\ -C_{n\beta} & C_{n\zeta} & (i_C s - C_{nr})s \end{vmatrix} \tag{23}$$

$$D_6' = \begin{vmatrix} 2\mu s - C_{y\beta} & -(C_{yp}s + C_{L0}) & 0 \\ -C_{l\beta} & i_A s^2 - C_{lp}s & C_{l\zeta} \\ -C_{n\beta} & -(i_E s^2 + C_{np}s) & C_{n\zeta} \end{vmatrix} \tag{24}$$

Since $D(s)$ and $D'(s)$ are the stability quartics in each case and $D(s)=0$ and $D'(s)=0$ are the characteristic equations of the longitudinal and lateral stability respectively, the poles of the airplane transfer function $G_a(s)$ are given by the roots of the characteristic equations.

Nevertheless, as shown in Eq. (1)~(6), all coefficients of the characteristic equations consist of the stability derivatives and the mass factors in non-dimensional form. Therefore, the characteristic roots or accordingly the poles of the transfer functions vary considerably in accordance with the flight conditions. In the first place, therefore, these variations of the poles must be investigated to facilitate the subsequent analysis.

The predictable changes of the flight conditions and accordingly the variations of coefficients are as follows:

1. Effect of altitude change ·····μ, i_A, i_B, i_C, i_E
2. Effect of c. g. position change ·····$C_{m\alpha}$
3. Effect of steady lift coefficient change ·····$C_{l\beta}$, C_{lr}, C_{np}

In addition to these factors, the change of stability derivatives due to changes in the airplane velocity and so on will be predicted, but they are neglected in this analysis for the sake of simplicity. Moreover, it is assumed that the compressibility effect of air is not so remarkable as shown in the example of numerical calculation.

When the equations of motion (1)~(6) are used exactly, it is extremely troublesome to calculate the roots of the characteristic equations, because they are quartics respectively. Therefore, in order to determine the variations of these roots the following approximate equations have been employed for calculating each mode of motion.

For instacce, in the case of the short period mode of longitudinal stability, the forward velocity increment $\hat{u}$ and the X-force equation can be neglected as an approximation in the equation of motion, therefore

$$(2\mu D - C_{z\dot{\alpha}} \cdot D - C_{z\alpha})\,\alpha - (2\mu + C_{zq})\,q = C_{z\eta} \cdot \eta \tag{25}$$

$$-(C_{m\dot{\alpha}} \cdot D + C_{m\alpha})\,\alpha + (i_B D - C_{mq})\,q = Cm_{\eta} \cdot \eta \tag{26}$$

accordingly, the characteristic equation is

$$\Delta = \begin{vmatrix} 2\mu s - C_{z\dot{\alpha}} \cdot s - C_{z\alpha} & -(2\mu + C_{zq}) \\ -(C_{m\dot{\alpha}} \cdot s + C_{m\alpha}) & i_B s - C_{mq} \end{vmatrix} = 0 \tag{27}$$

Since Eq. (27) is the quadratic equation about s, it is easy to calculate the change of roots accompanying the variations of the coefficients.

Similarly, the other mode of motion can be calculated in the following manner. In the phugoid mode, the angle of attack α term and the pitching moment equation can be neglected approximately,

$$(2\mu D - C_{xu})\,\hat{u} + C_{L0}\theta = 0 \tag{28}$$

$$(2C_{L0} - C_{zu})\,\hat{u} - (2\mu + C_{zq})\,D\theta = C_{z\eta} \cdot \eta \tag{29}$$

In the rolling mode, the terms of the sideslip angle β and the yawing angle ψ and the side-force equation and the yawing moment equation can be neglected,

$$(i_A D - C_{lp})\,p = Cl_{\xi} \cdot \xi + C_{l\zeta} \cdot \zeta \tag{30}$$

In the lateral oscillation or "Dutch-Roll" mode, the yawing angle ψ is approximately equal to $-\beta$ and the side-force equation can be neglected,

$$(i_E D^2 + C_{lr} \cdot D - C_{l\beta})\,\beta + (i_A D - C_{lp})\,p = Cl_{\xi} \cdot \xi + C_{l\zeta} \cdot \zeta \tag{31}$$

$$-(i_C D^2 - C_{nr} D + C_{n\beta})\,\beta + (i_E D + C_{np})\,p = C_{n\xi} \cdot \xi + C_{n\zeta} \cdot \zeta \tag{32}$$

In the spiral mode, the higher terms of the characteristic equation can be neglected,

$$\{(2\mu - C_{yr})(C_{l\beta} C_{np} - C_{n\beta} C_{lp}) - C_{L0}(i_C C_{l\beta} + i_E C_{n\beta})\}\,D + C_{L0}(C_{l\beta} \cdot C_{nr} - C_{n\beta} \cdot C_{lr}) = 0 \tag{33}$$

The numerical values which are used in the subsequent calculations are listed as follows: (at cruising condition)

W	= 100,000 lb	S	= 1667 ft^2
b	= 108 ft	$\bar{c}$	= 15.4 ft
A	= 7	Λ	= 30°
V	= 500 mph	$Alt._{\text{cruise}}$	= 30,000 ft
$C_{L0\,\text{cruise}}$	= 0.25	C_{D0}	= 0.0188

$C_{xu} = -0.0376$	$C_{x\alpha} = 0.14$
$C_{zu} = 0$	$C_{z\alpha} = -4.90$
$C_{mu} = 0$	$C_{z\dot{\alpha}} = 0$
$C_{mq} = -22.9$	$C_{m\alpha} = -0.488$
$C_{zq} = 0$	$C_{m\dot{\alpha}} = -4.20$
$\mu_{\text{longitudinal}} = 272$	$i_B = 1900$
$C_{y\beta} = -0.168$	$C_{yp} = 0$
$C_{yr} = 0.192$	$C_{lp} = -0.43$
$C_{l\beta} = -0.047$	$C_{lr} = 0.070$
$C_{n\beta} = 0.0385$	$C_{np} = -0.017$
$C_{nr} = -0.117$	
$\mu_{\text{lateral}} = 38.8$	$i_A = 3.69$
$i_C = 9.22$	$i_E = -0.39$
$C_{z\eta} = -0.24$	$C_{m\eta} = -0.72$
$C_{l\xi} = -0.065$	$C_{n\xi} = 0.005$
$C_{l\zeta} = 0.003$	$C_{n\zeta} = -0.040$

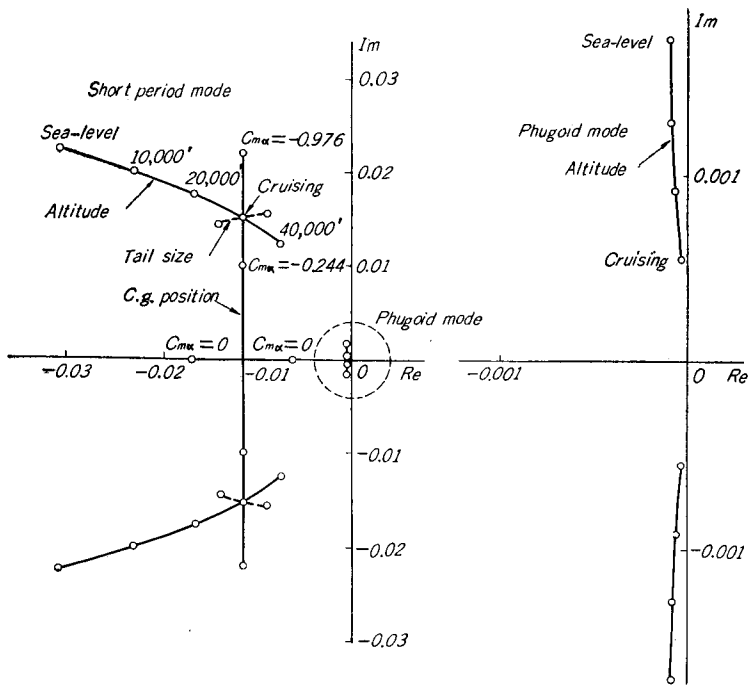

Fig. 2. The variation of the locus of roots with the flight conditions. (longitudinal case)

The root locus diagrams for each mode of motion attendant on changes in these coefficients are shown in Fig. 2 (longitudinal case) and Fig. 3 (lateral case).

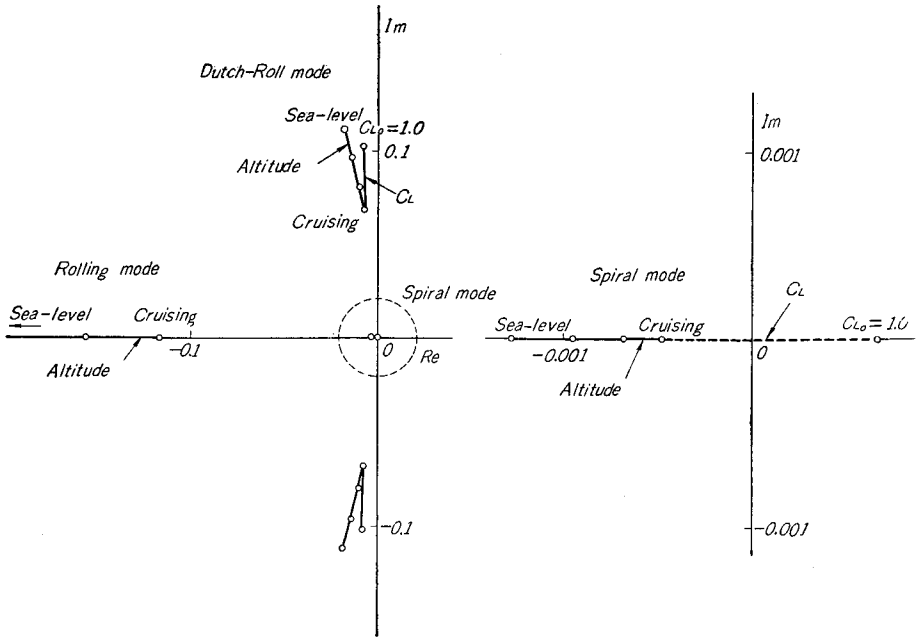

Fig. 3. The variation of the locus of roots with the flight conditions. (lateral case)

From these root locus the following conclusions can be derived.

1. The influence of an altitude increase is the most remarkable among the changes in flight conditions, and it has a destabilizing inclination in all cases. Therefore, in general, it is supposed that the stability is lowest at cruising conditions.
2. The destabilizing inclination accompanying the altitude increase is largest in the short period mode among all modes of motion. The dotted line in Fig. 2 shows the change of stability which has been calculated for ± 40 percent change of horizontal tail volume ratio. In comparison with this case, it is understood that the effect of altitude increase is very notable.

Referring to the above-mentioned results, therefore, the subsequent calculation has been made using the numerical values at the cruising condition.

The transfer functions of the airplane in each case can be determined as follows:

(1) Logitudinal system

$$G_{\alpha\eta}(s) = \frac{-0.00044(s+0.87)(s+0.0000343+0.0000635i)(s+0.0000343-0.000635i)}{(s+0.01162+0.01515i)(s+0.01162-0.01515i)(s+0.0000302+0.000545i)} \times \overline{(s+0.0000302-0.000545i)} \tag{34}$$

$$G_{\theta\eta}(s) = \frac{-0.000378(s+0.0001)(s+0.0087)}{(s+0.01162+0.01515i)(s+0.01162-0.01515)(s+0.0000302+0.000545i)} \times \overline{(s+0.0000302-0.000545i)} \tag{35}$$

(2) Lateral system

$$G_{\beta\xi}(s) = \frac{-0.0013(s+0.00470)(s+0.114)}{(s+0.00048)(s+0.1178)(s+0.00723+0.0682i)(s+0.00723-0.0682i)} \tag{36}$$

$$G_{\phi\xi}(s) = \frac{-0.0177(s+0.00712+0.0610i)(s+0.00712-0.0610i)}{(s+0.00048)(s+0.1178)(s+0.00723+0.0682i)(s+0.00723-0.0682i)} \tag{37}$$

$$G_{\psi\xi}(s) = \frac{0.0013(s-0.038)(s+0.0571+0.0349i)(s+0.0571-0.0349i)}{s(s+0.00048)(s+0.1178)(s+0.00723+0.0682i)(s+0.00723-0.0682i)} \tag{38}$$

$$G_{\beta\zeta}(s) = \frac{0.0044(s-0.00043)(s+0.117)}{(s+0.00048)(s+0.1178)(s+0.00723+0.0682i)(s+0.00723-0.0682i)} \tag{39}$$

$$G_{\phi\zeta}(s) = \frac{0.00128(s-0.233)(s+0.175)}{(s+0.00048)(s+0.1178)(s+0.00723+0.0682i)(s+0.00723-0.0682i)} \tag{40}$$

$$G_{\psi\zeta}(s) = \frac{-0.0044(s+0.117)(s+0.000433+0.012i)(s+0.000433-0.0121i)}{s(s+0.00048)(s+0.1178)(s+0.00723+0.0682i)(s+0.00723-0.0682i)} \tag{41}$$

In comparison with these transfer functions, several cases which have been calculated by the approximate equations (25)~(33) are shown as follows:

(1) Short period mode

$$G_{\alpha\eta}(s) = \frac{-0.00044(s+0.87)}{(s+0.01162+0.01515i)(s+0.01162-0.01515i)} \tag{42}$$

$$G_{\theta\eta}(s) = \frac{-0.00038(s-0.0087)}{s(s+0.01162+0.01515i)(s+0.01162-0.01515i)} \tag{43}$$

(2) Lateral oscillation mode

$$G_{\beta\zeta}(s) = -G_{\psi\zeta}(s) = \frac{0.0044(s+0.116)}{(s+0.115)(s+0.0077+0.066i)(s+0.0077-0.066i)} \tag{44}$$

The approximate functions will be found to be those in which the zeros and poles of the same order have been cancelled out.

(2) Calculation of the transfer function of a human-pilot $G_h(s)$

For simplicity, it is assumed that the pilot makes a displacement control. In other words, his control movement will be applied in proportion to the angular displacement of the airplane output motion for decreasing the transient motion.

The theoretical and reasonable form of $G_h(s)$ as a control element of an automatic control system, will be difficult to determine but on the stability analysis of an airplane, it will be sufficient to assume several simple forms, because the pilot acts only to damp out the transient motion. In this paper, therefore, the transfer function $G_h(s)$ has been assumed as follows:

$$G_h(s) = K_0 \tag{45}$$

$$= \frac{K_0}{1+\tau_1 s} \tag{46}$$

$$= \frac{K_0 e^{-\tau_2 s}}{1+\tau_1 s} \tag{47}$$

i.e. Eq. (45) is the case in which an ideal feedback control of gain K_0 is assumed, Eq. (46) is the case in which the human muscular lag time is considered and Eq. (47) is the case in which the muscular lag time and the human response time lag are considered. In the above equations, τ_1 and τ_2 are the time constants and the numerical values are about 0.2~0.5 sec.. Moreover, the gain K_0 is variable and in some cases zero because of the human-pilot characteristics.

Since, in Eq. (47), it is difficult to express the response time lag term $e^{-\tau_2 s}$ graphically in that form, it is necessary to transform it to the polynomial form using the following approximation. In this case, τ_2 and s (which corresponds to $i\omega$ in the frequency domain) are small, therefore

$$e^{-\tau_2 s} \cong 1-\tau_2 s+\frac{\tau_2^2 s^2}{2} = \frac{1}{2}\{\tau_2 s-(1+i)\}\{\tau_2 s-(1-i)\} \tag{48}$$

Therefore, Eq. (47) may be expressed approximately,

$$G_h(s) = \frac{\{\tau_2 s-(1+i)\}\{\tau_2 s-(1-i)\}}{2(1+\tau_1 s)} \tag{49}$$

To compare with the original function, the frequency response diagrams of these functions are shown in Fig. 4, where $\tau_1=0.125$ sec. and $\tau_2=0.25$ sec. are assumed. It is supposed that this approximation will not cause too much error in the calculation, because the highest angular frequency ω of the airplane motion, for instance the short period mode or Dutch-Roll mode, is at most 1~2 r/s as shown in Fig. 4.

Moreover, it is necessary to make the coefficients of the function $G_h(s)$ as well as of $G_a(s)$ dimensionless before the calculation. The aerodynamic times are $t^*=0.0105$ sec. and $t^*=0.0737$ sec. for longitudinal and lateral cases respectively, therefore, if $\tau_1=\tau_2=0.25$ sec. are assumed, Eq. (46) will be

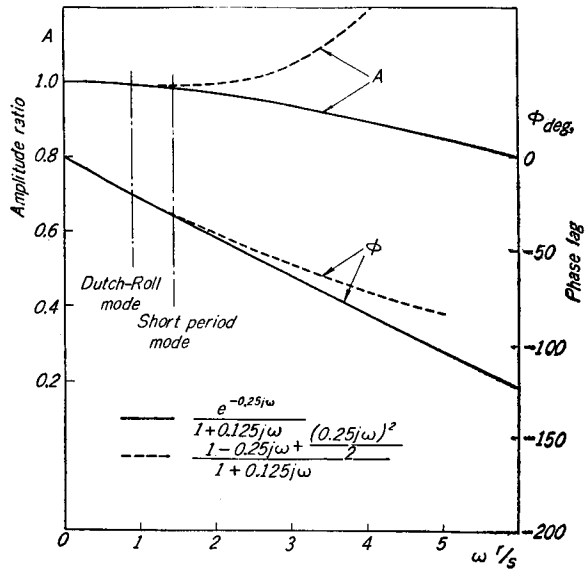

Fig. 4. Frequency response for pilot reaction time and muscular lag.

$$G_h(s) = \frac{0.042\,K_0}{s+0.042} \tag{50}$$

$$= \frac{0.295\,K_0}{0+0.295} \tag{51}$$

In the same way, Eq. (49) will be

$$G_h(s) = \frac{11.9\,K_0\{s-0.042(1+i)\}\{s-0.042(1-i)\}}{s+0.042} \tag{52}$$

$$= \frac{1.7\,K_0\{s-0.295(1+i)\}\{s-0.295(1-i)\}}{s+0.295} \tag{53}$$

In each case, the former is for the longitudinal case and the latter for the lateral case respectively.

3. Root-Locus of the Closed-Loop System

The root locus of the characteristic equation of a closed-loop system can be determined graphically by the Evan's Method. The zeros and poles of the open-loop system have already been determined in the last section. Several root locus diagrams of the representative modes of motion are shown in Fig. 5~Fig. 10. The variable in this root locus is the gain K_0.

Fig. 5 and Fig. 6 are the cases of longitudinal stability, where the output motions of the airplane are the angle of attack α and the pitching angle θ, and

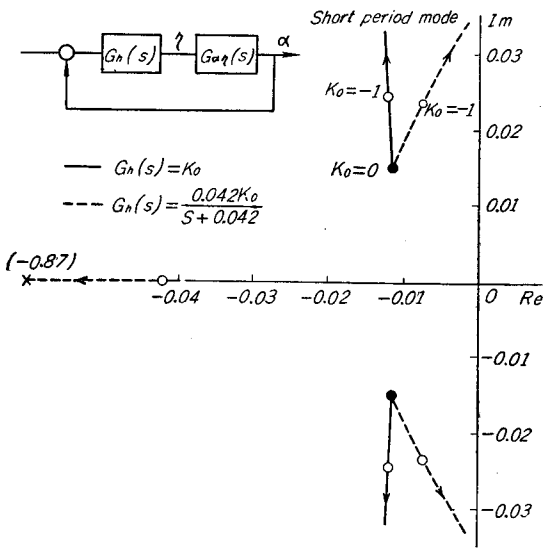

Fig. 5. Root-locus plot in which the output motion is the angle of attack α and the pilot control is the elevator ongle η. (longitudinal case)

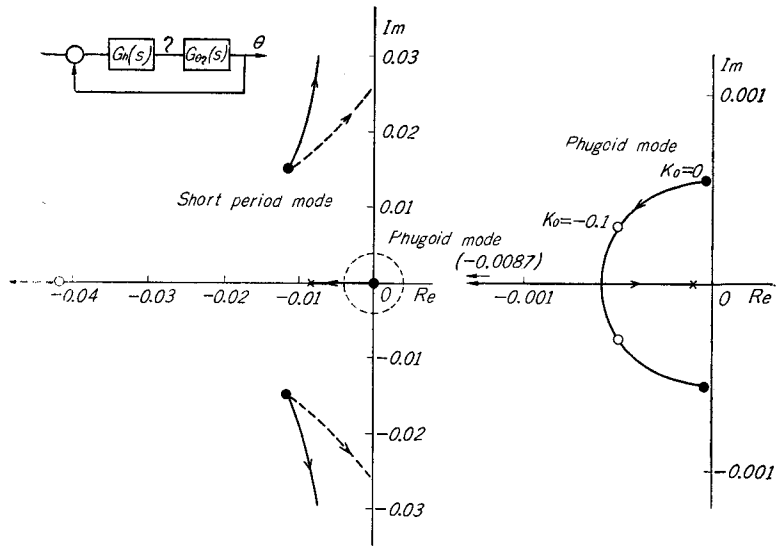

Fig. 6. Root-locus plot in which the output motion is the pitching angle θ and the pilot control is the elevator angle η. (longitudinal case)

the pilot controls the elevator angle η. The characteristics of the short period mode are expressed in both cases, but the phugoid mode does not appear in the case of the angle of attack α.

Fig. 7, Fig. 8 and Fig. 9 are the cases of lateral stability. The output motions of the airplane are the sideship angle β, the rolling angle ϕ and the yawing angle ψ, and the pilot controls are the aileron angle ξ and the rudder angle ζ. Therefore, these diagrams are the representative cases for suitable combinations of some elements. The stability characteristics of the rolling mode, Dutch-Roll mode and spiral mode are shown in these diagrams. The photographs (Photo. 1~18) illustrate the forms of the transient motion corresponding to each gain K_0 which is shown in those diagrams. These are photographs taken of the oscillograms calculated by the analog computor.

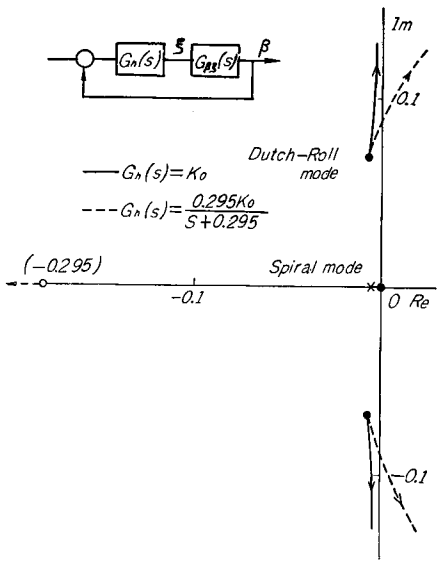

Fig. 7. Root-locus plot in which the output motion is the sideslip angle β and the pilot control is the aileron angle ξ. (lateral case)

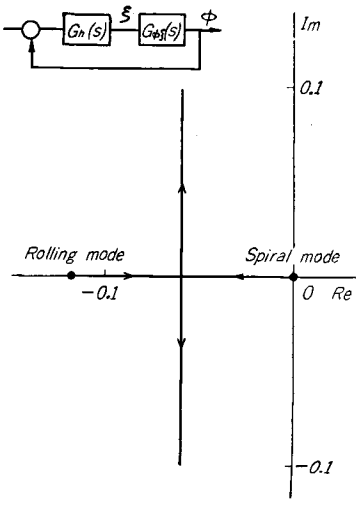

Fig. 8. Root-locus plot in which the output motion is the rolling angle ϕ and the pilot control is the aileron angle ξ. (lateral case)

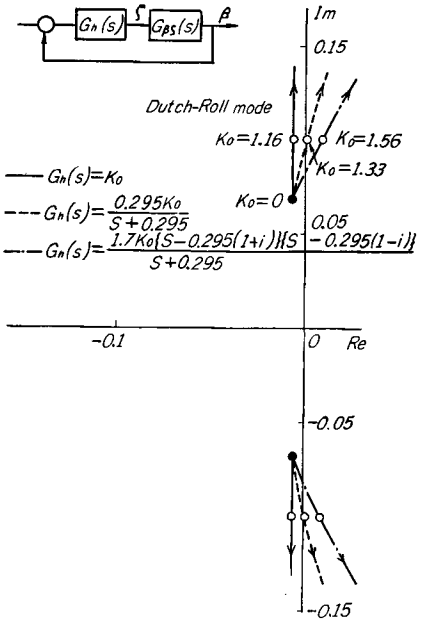

Fig. 9. Root-locus plot in which the output motion is the sideslip angle β and the pilot control is the rudde rangle ζ. (lateral case)

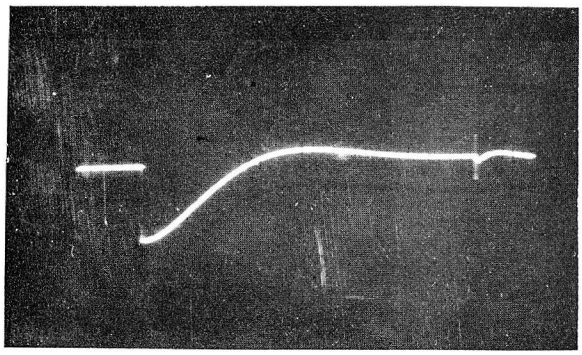

Photo. 1. Short period mode. (transfer function: $G_{\alpha\eta}(s)$, gain: $K_0=0$)

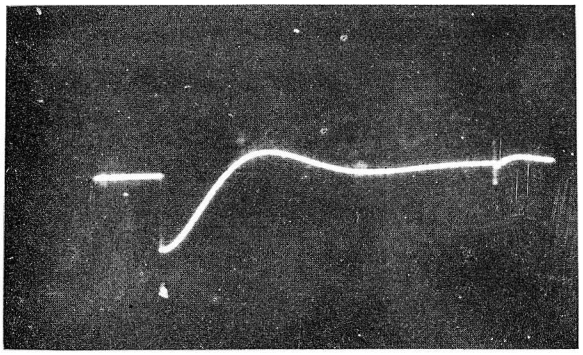

Photo. 2. Short period mode. (transfer function: $G_{\alpha\eta}(s)$, gain; $K_0=-1.0$ (ideal))

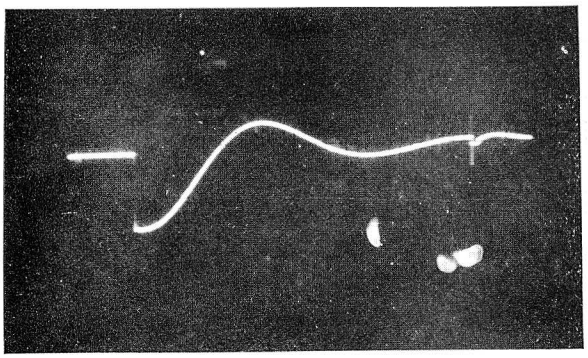

Photo. 3. Short period mode. (transfer function: $G_{\alpha\eta}(s)$, gain; $K_0=-1.0$ (muscular time lag))

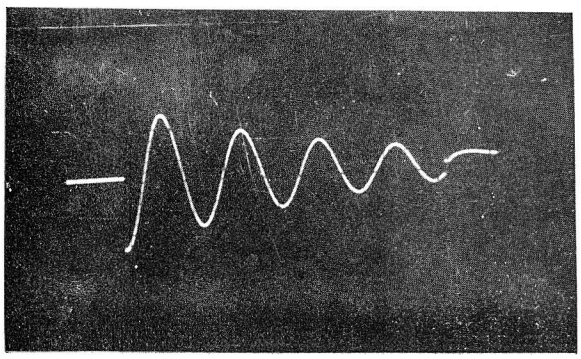

Photo. 4. Phugoid moee. (transfer function: $G_{\theta\eta}(s)$, gain: $K_0=0$)

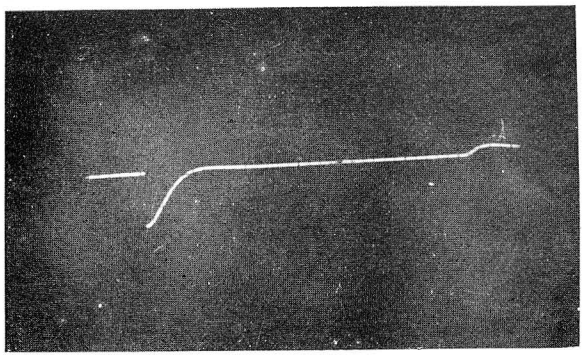

Photo. 5. Phugoid mode. (transfer function; $G_{\theta\eta}(s)$, gain: $K_0=-0.1$ (ideal))

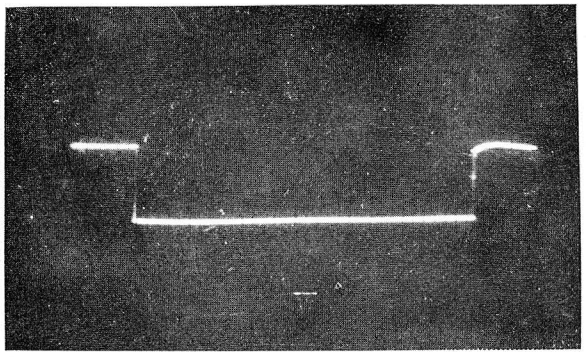

Photo. 6. Spiral mode. (transfer function: $G_{\beta\xi}(s)$, gain; $K_0=0$)

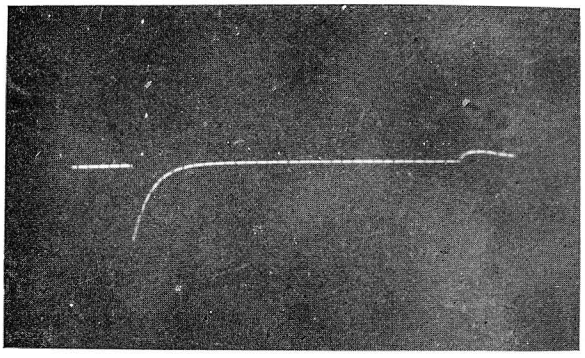

Photo. 7. Rolling mode- (transfer function; $G_{\phi_2^1}(s)$, gain; $K_0=0$)

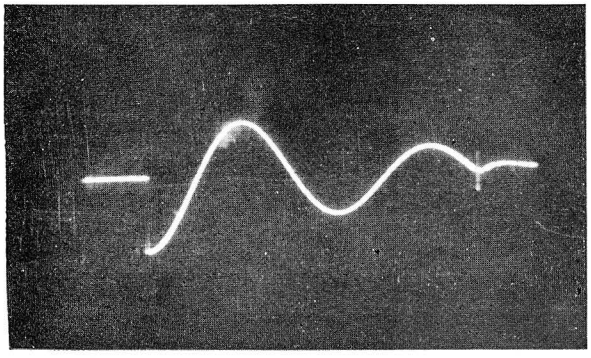

Photo. 8. Dutch-Roll mode. (transfer function $G_{\beta\zeta}(s)$, gain: $K_0=0$)

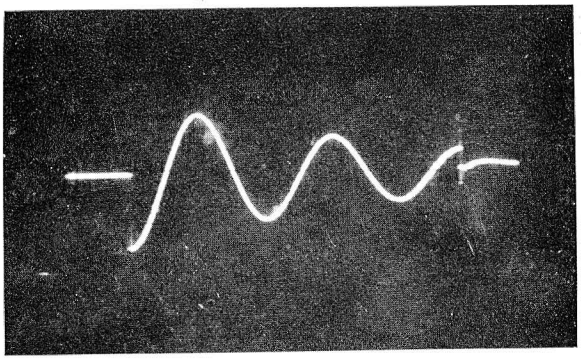

Photo. 9. Dutch-Roll mode. (transfer function: $G_{\beta\zeta}(s)$, gain: $K_0=1.0$ (ideal))

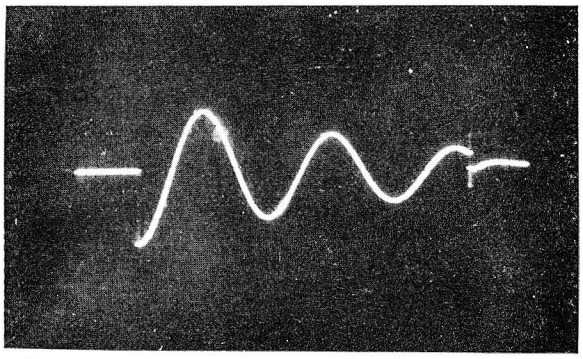

Photo. 10. Dutch-Roll mode. (transfer function: $G_{\beta\zeta}(s)$, gain: $K_0=1.2$ (ideal))

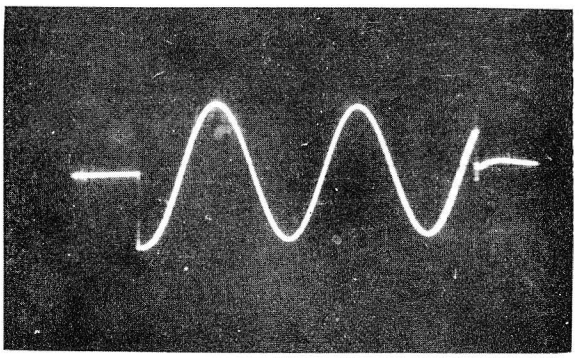

Photo. 11. Dutch-Roll mode. (transfer function: $G_{\beta\zeta}(s)$, gain: $K_0=1.0$ (muscular time lag))

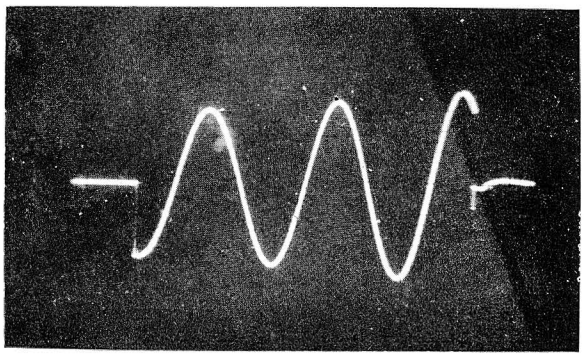

Phato. 12. Dutch-Roll mode. (transfer function: $G_{\beta\zeta}(s)$, gain: $K_0=1.5$ (muscular time lag))

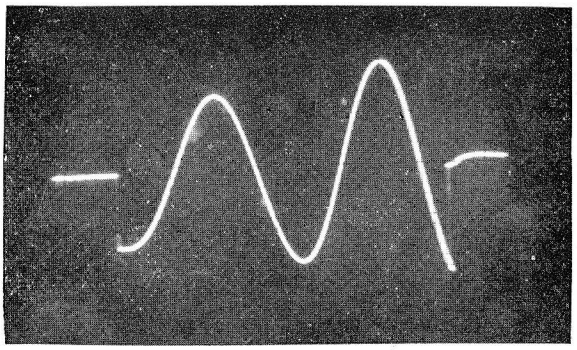

Photo. 13. Dutch-Roll mode. (transfer function; $G_{\beta\zeta}(s)$, gain: $K_0=1.0$ (muscular, response time lag))

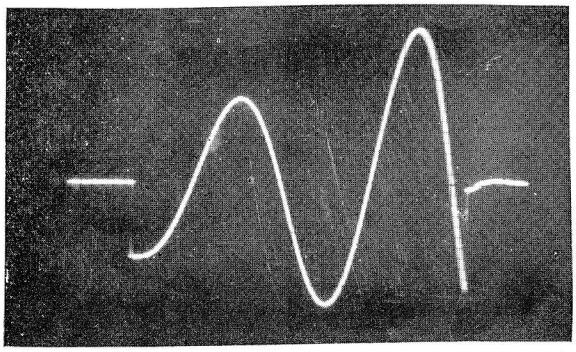

Photo. 14. Dutch-Roll mode. (transfer function: $G_{\beta\zeta}(s)$, gain: $K_0=1.5$ (muscular, response time lag))

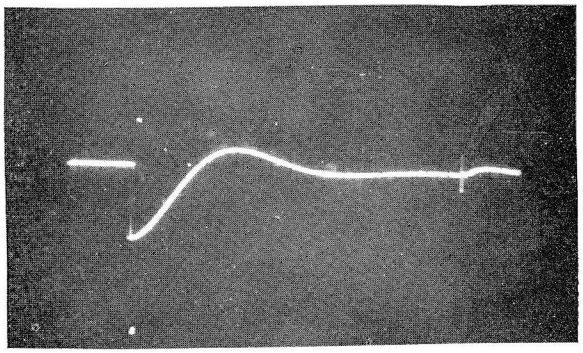

Photo. 15. Dutch-Roll mode. (rate control) (transfer function: $G_{\beta\zeta}(s)$, gain: $K_0=$ 10 (ideal))

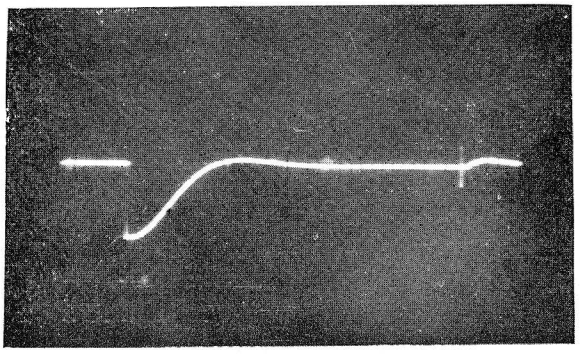

Phota. 16. Dutch-Roll mode. (rate control) (transfer function: $G_{\beta\zeta}(s)$, gain: $K_0=$ 15 (ideal))

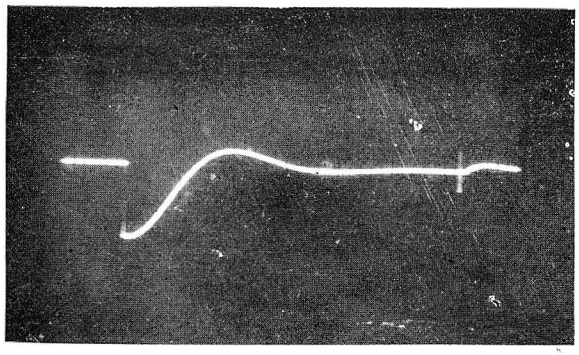

Photo. 17. Dutch-Roll mode. (rate control) (transfer function : $G_{\beta\zeta}(s)$, gain : K_0= 10 (muscular time lag))

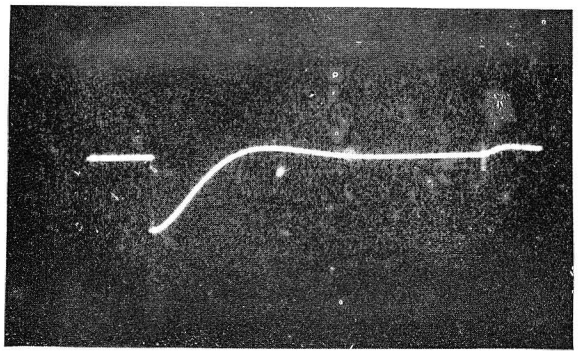

Photo. 18. Dutch-Roll mode. (rate control) (transfer function : $G_{\beta\zeta}(s)$, gain : K_0= 15 (muscular time lag))

From the above-mentioned results, the following conclusion can be derived.

1. As shown in Fig. 6 and Fig. 7, it is obvious that the phugoid mode or the spiral mode can quite easily be stabilized by the control movement of a human-pilot, even if it is unstable. The time lag characteristics with a human-pilot control scarcely affect the stabilized motion.
2. On the contrary, as shown in Fig. 5 and Fig. 9, the short period mode or the Dutch-Roll mode cannot easily be stabilized. In other words, these modes of motion will not be easily damped out by the feedback control movement of a human-pilot. In particular, when the time lag characteristics of a human-pilot control are influential, they produce rather a destabilizing tendency. It will therefore be necessary to provide a yaw damper or pitch damper for airplanes of very low damping in such modes of motion.

In the above-mentioned numerical calculation, the short period mode of this airplane is still sufficiently stable at the cruising condition as shown in the photograph, even though the damping is much lower than at the low altitude condition. Therefore there will be no need for human-pilot control in this case.

Nevertheless, on the other hand, the Dutch-Roll mode of this airplane shows such a low damping oscillation that it will be necessary to decrease the transient

mation more quickly by some means.

In the above-mentioned analysis, however, it has been assumed that a human-pilot makes a displacement control only, but in actual practice both displacement control and rate control may be combined. If the human-pilot control is assumed to be pure rate control, it is supposed that the stabilizing efficiency of his control will be greatly increased over that of displacement control as shown in Fig. 10. Therefore, the control effectiveness of a human-pilot may be greatly improved by increasing the degree of rate control as much as possible.

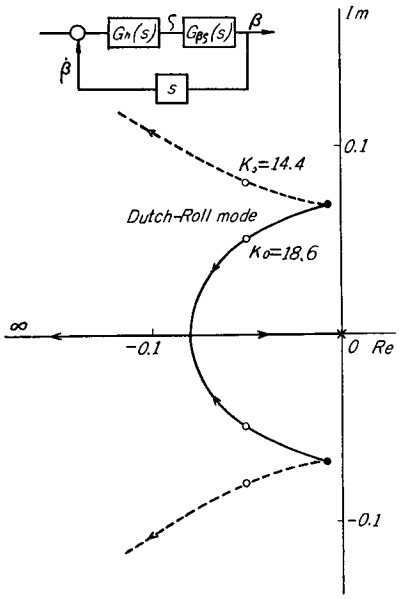

Fig. 10. Root-locus plot of ideal rate control in the same case of Fig. 9.

4. Concluding Remarks

A method for calculating the dynamic stability of a human-piloted airplane by the Evans's "Root-Locus Method" has been presented.

Generally, the root locus diagrams of the characteristics equation of a open-loop system or a closed-loop system are undoubtedly very advantageous for the stability analysis of such a dynamic system as an airplane. Moreover, when an airplane is treated as a closed-loop system which contains a human-pilot as one feedback element, not only the transient motion characteristics of the airplane but the control ability of the human-pilot to damp out the residual motion are conveniently investigated. For a more strict analysis, however, a more detailed and exact expression for the transfer function, such as that for a human-pilot, should be developed.

References

1) B. Etkin; "Dynamics of Flight" John Wiley & Sons, (1959).
2) J. L. Decker; Jour. Aero. Sci., Vol. 23, No. 8 (1956).
3) R. S. White; Jour. Aero. Sci., Vol. 17, No. 3 (1950).
4) W. Bollay; Jour. Aero. Sci., Vol. 18, No. 9 (1951).
5) D. Graham and R. C. Lathrop; Aero. Eng. Rev., Vol. 14, No. 10 (1955).
6) H. Maeda; THIS MEMOIRS, **22**, 301 (1960).